Molecular structure of the lecithin ripple phase

Alex H. de Vries*, Serge Yefimov, Alan E. Mark, and Siewert J. Marrink

Molecular Dynamics Group, Department of Biophysical Chemistry, University of Groningen, Nijenborgh 4, 9747 AG Groningen, The Netherlands

Edited by Michael Levitt, Stanford University School of Medicine, Stanford, CA, and approved February 23, 2005 (received for review November 5, 2004)

Molecular dynamics simulations of lecithin lipid bilayers in water as they are cooled from the liquid crystalline phase show the spontaneous formation of rippled bilayers. The ripple consists of two domains of different length and orientation, connected by a kink. The organization of the lipids in one domain of the ripple is found to be that of a splayed gel; in the other domain the lipids are gel-like and fully interdigitated. In the concave part of the kink region between the domains the lipids are disordered. The results are consistent with the experimental information available and provide an atomic-level model that may be tested by further experiments.

molecular dynamics simulation | structural model

Lipid bilayers are studied widely as models for biological membranes (1). Biological membranes have many components. The complexity of the biological membrane facilitates a wide range of functionalities. Among these, order–disorder transitions within the lipid matrix are believed to play a crucial role in the regulation of protein function (2). Single-component phosphatidylcholine (lecithin) lipid aggregates in water, however, already show rich phase behavior (3). Upon cooling lecithin bilayers from the liquid crystalline (L_α) state to a temperature below the main transition temperature, x-ray studies have revealed the formation of rippled bilayers (4–8). This phase is denoted $P_{\beta'}$. Upon further cooling below the pretransition temperature, a gel phase is found in which the lipid tails are fully stretched and ordered in a hexagonal array, with a uniform tilt with respect to the bilayer normal. This phase is denoted $L_{\beta'}$. X-ray studies of the $P_{\beta'}$ phase have been used to obtain the ripple length (λ_r), the stacking repeat distance (d), and the oblique angle (γ), as shown in Fig. 1 (5). The ripple is asymmetric (sawtooth-like) and consists of a major domain (*M* domain) and a minor domain (*m* domain) (6), connected by a kink. Several theories have been developed to explain the appearance of this kink. These theories either emphasize the packing frustration caused by the difference in steric requirements between the head groups and the tails of the lipids or emphasize the interaction between neighboring bilayers (for reviews, see refs. 5 and 9). Because the ripple phase is intermediate between the fluid and gel phases, study of its properties contributes to our understanding of the balance of forces within the lipid matrix and the resulting molecular organization. These insights are likely to be relevant to order–disorder transitions in a wider sense.

The organization of the lipids in the domains of the ripple is unknown (10). It is generally agreed that the thickness of the lipid layer differs in the two domains (6). From x-ray scattering data the thickness of the bilayer in the *M* domain is found to be comparable to that found in the $L_{\beta'}$ phase. The thickness of the bilayer in the *m* domain is found to be considerably smaller. It is consistent with the thickness found in the L_α phase, but there is no clear evidence that the lipid tails show a level of conformational disorder comparable to that in the L_α state. There is experimental evidence for a high degree of tail stretching throughout the ripple phase from Fourier transform infrared (11) and solid-state ^{13}C-NMR (12) measurements. The presence of a sharp peak in the wide-angle x-ray scattering (WAXS) region of the powder spectrum indicates that a sizeable part of the structure shows short-range order (13). In contrast, the presence of a considerable fraction of significantly more mobile lipids has been inferred from solid-state ^{13}C-NMR (12) and fluorescence photobleaching recovery (14) experiments.

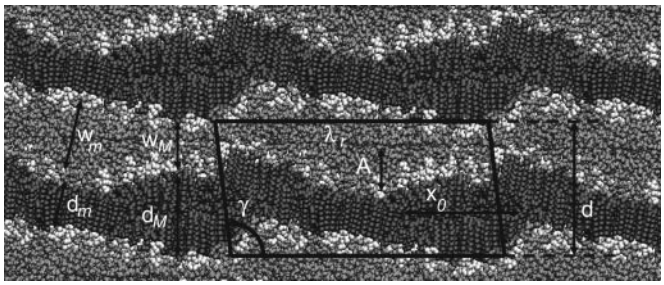

Fig. 1. Characteristics of the ripple phase are shown. λ_r, ripple length; d, stacking repeat distance; γ, oblique angle; x_0, projection of *M* domain on ripple vector; A, ripple amplitude. The triclinic unit cell is shown as a projection on a periodically replicated snapshot taken from a MD simulation. Lipid head groups are shown in white, lipid tails are in gray. Water is shown in light gray. Note the differences in thickness of the lipid domains (d_M and d_m) and water layers between the lipid domains (w_M and w_m).

Here, we report low-temperature structures of phosphatidylcholine lipid bilayers in water obtained from molecular dynamics (MD) simulations. MD simulations are one means to investigate molecular organization in atomic detail and have been used extensively to study the properties of lipid bilayers, predominantly in the L_α state (15). Some studies on the $L_{\beta'}$ state (16, 17) have been reported, but these have been biased in the sense that starting structures were taken from low-temperature crystal structures. The structures presented here were formed spontaneously from the L_α state after cooling the system. To our knowledge, a ripple phase has never been reported in simulations using atomistic lipid models. A rippled bilayer has been reported with a coarse-grained lipid model (18). In this ripple phase, thicker and thinner domains alternate but they show a symmetric peristaltic profile along the ripple vector, rather than the sawtooth profile inferred from x-ray scattering data.

Methods

Simulations were performed by using anisotropic pressure coupling (P = 1 bar) with the force field as described for system F in ref. 19. This force field describes lipid molecules and water molecules at the atomistic level. Methyl and methylene groups are described by using a so-called united atom representation, in which the H atoms connected to the C atoms are not treated explicitly. Interactions between atoms were calculated by using a twin-range cut-off scheme. Interactions between particles within the short-range cut-off of 1.0 nm were updated every step. Interactions between particles within the long-range cut-off of 1.4 nm were updated every 10 steps. The cut-off for the Lennard–Jones interactions was 1.0 nm. The cut-off for the electrostatic interactions, evaluated by using the reaction-field

This paper was submitted directly (Track II) to the PNAS office.

Abbreviations: L_α, liquid crystalline; *M* domain, major domain; *m* domain, minor domain; WAXS, wide-angle x-ray scattering; MD, molecular dynamics; DPPC, dipalmitoylphosphatidylcholine.

*To whom correspondence should be addressed. E-mail: a.h.de.vries@rug.nl.

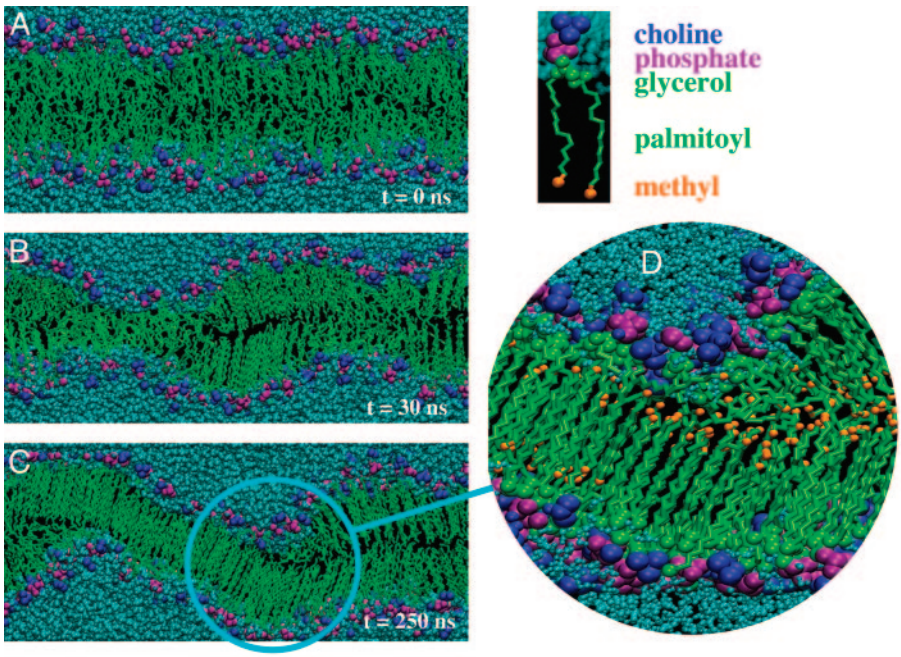

Fig. 2. Ripple phase structure from MD simulation. The unit cell contained 256 DPPC lipid molecules and 23 water molecules per lipid. This simulation was run at 283 K. A cut through the system is shown. The horizontal is the ripple vector direction; the vertical is the stacking direction. The color scheme is shown in the upper right. In *A–C* the terminal methyl groups are not colored orange. (*A*) The initial structure (t = 0 ns) taken from an equilibrated L_α simulation. (*B*) An intermediate structure (t = 30 ns). (*C*) A fully formed ripple structure (t = 250 ns). (*D*) Close-up of *C*. From left to right along the ripple vector, the interdigitation in the *m* domain and the highly disordered acyl chains in the concave part of the kink region are seen. In the lower leaflet, the orientation of the acyl chains with respect to the ripple vector is seen to change gradually.

correction of Tironi *et al.* (20), was 1.4 nm. Periodic boundary conditions were used. Most simulations used a fully flexible (triclinic) simulation box. All simulations were performed with the GROMACS code (21), versions 3.0.5 and 3.1.4. In general, a time step of 5 fs was used. The use of different coupling schemes for pressure coupling [Berendsen *et al.* (22) and Parrinello and Rahman (23) barostats] and for temperature coupling [Berendsen *et al.* (22) and Nosé–Hoover (24) thermostats] was tested and was not found to influence the results. A number of simulations accounting for long-range electrostatic interactions by using the particle mesh Ewald (PME) technique were also performed for comparison. The use of PME did not affect the nature of the structures formed.

WAXS data were generated from a snapshot obtained from the simulations. The spectrum was calculated from the positions of all lipid atoms in the unit cell of a representative configuration of the system by using the formula:

$$I(\boldsymbol{q}) = \sum_{\mathrm{i}} \sum_{\mathrm{j}} n_{\mathrm{i}} n_{\mathrm{j}} \cos(-2\pi[\boldsymbol{q}\cdot(\boldsymbol{r}_{\mathrm{j}} - \boldsymbol{r}_{\mathrm{i}})]).$$

$I(\boldsymbol{q})$ is the real part of the intensity in reciprocal space, $\boldsymbol{q}$ is a 3D vector in reciprocal space, $(\boldsymbol{r}_{\mathrm{j}} - \boldsymbol{r}_{\mathrm{i}})$ is the vector between atoms i and j in real space, and n_{i} and n_{j} are the number of electrons associated with atoms i and j, respectively. The z axis in real space was chosen to be the ripple stacking direction. The transform from real space to reciprocal space was performed on the fly and stored on a grid. The spacing of the grid used was 0.1 nm^{-1} in all directions. Angle-resolved spectra were then generated from the 3D data. The data were mapped on a 2D grid by projecting the $I(\boldsymbol{q})$ on q_z and on the plane perpendicular to q_z, $q_{\mathrm{r}} = (q_{\mathrm{x}}^2 + q_{\mathrm{y}}^2)^{1/2}$.

Results

Fig. 2 *A–C* shows a series of snapshots taken from a MD simulation of a dipalmitoylphosphatidylcholine (DPPC) bilayer in water after instantaneously cooling the system to a temperature of 283 K, which is below the experimental transition temperature of 315 K for DPPC (3). The starting structure is taken from a simulation at a temperature of 323 K, at which the DPPC bilayer is in the L_α phase (Fig. 2*A*). During the simulations a ripple profile appears as soon as condensation nuclei consisting of lipids with stretched acyl chains are formed (Fig. 2*B*). This process occurs on a time scale of several nanoseconds. The stretched chains of the lipids in these condensation nuclei are splayed along the ripple vector. A domain with disordered chains is formed in between the ordered domains. This disordered domain is tilted with respect to the ordered domains and the chains in the disordered domain are partly interdigitated. Further interdigitation and ordering into a fully interdigitated gel ($L_{\beta I}$) domain takes much longer, tens to hundreds of nanoseconds in our simulations. Resolving defects in the uninterdigitated gel-like domain is also a slow process. Eventually, the system evolves into an asymmetric ripple structure with two domains that differ in length and bilayer thickness (Fig. 2*C*). The two domains are connected by a kink. The majority of the lipids are seen to have fully stretched tails with only a few gauche defects located toward the end of the acyl chains. In the *M* domain, the two monolayers are separated from each other and the lipids are tilted with respect to the bilayer normal. The tilt with respect to the stacking vector along the ripple vector is not uniform. In the *m* domain, the lipid tails of the two monolayers are fully interdigitated and have a uniform tilt with respect to the stacking direction. The two domains as a whole are oriented differently with respect to the stacking direction, thus showing an asymmetric ripple profile (sawtooth). The change in orientation of the domains occurs over a few molecular diameters and is therefore seen as a kink.

Fig. 2*D* shows a close-up of the ripple structure at the end of the simulation, revealing the organization of the lipid molecules around the kink region. The tails of the lipids in the concave part

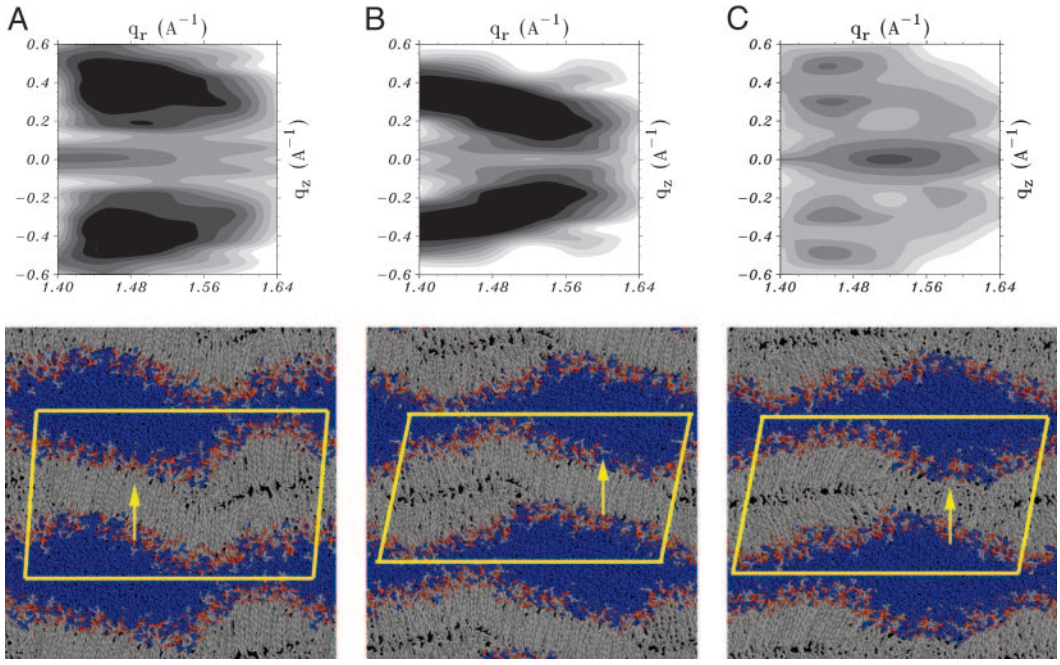

Fig. 3. Calculated WAXS intensities from (*Upper*) and snapshots of (*Lower*) DPPC ripple structures. The intensity is plotted as contours colored on a gray scale, using logarithmic procession of the levels. The levels are the same in all pictures, and the intensities were calculated from the positions of the same number of atoms. In the snapshots, Corey, Pauling, Kultun coloring is used, except for water, which is colored blue. The yellow lines show the projection of the unit cell on the x-z plane and the arrow indicates the *z* axis. (*A*) Ripple phase structure. (*B*) Ripple-like structure after partial melting of the *M* domain. (*C*) Ripple-like structure with an ordered *M* domain and liquid-like *m* domain.

of the kink are highly disordered, showing many gauche defects. The lipids in the kink region adopt conformations that are similar to the conformations lipids adopt in highly curved regions around water pores (25) and in a small vesicle (26). Ripple structures similar to those shown in Figs. 1 and 2 were found under many simulation conditions as long as the number of lipid molecules in the periodically repeated simulation cell was at least 128 (64 per monolayer). The length of the ripple depended strongly on the system size because initial ripple formation occurs faster than lipids are able to redistribute laterally between the ripple vector direction and the other lateral direction. The thickness of the domains and the lipid organization in the kink regions were nevertheless similar. Simulations with two bilayers in the periodic box also resulted in ripple structures (see Fig. 5, which is published as supporting information on the PNAS web site). In smaller systems, symmetric, peristaltic ripple structures like the ones described in ref. 18 were observed (Fig. 6, which is published as supporting information on the PNAS web site). Simulations were performed at several temperatures, starting from both L_α and L_β' structures, and at levels of hydration corresponding to fully hydrated L_α (23–30 water per lipid) and gel states (12–15 water per lipid), as well as intermediate hydrations. Whereas the nucleation of the *M* domain takes place within tens of ns, the formation of a fully interdigitated *m* domain (in the case of ripple formation) takes hundreds of ns. Running simulations at higher temperature, lower hydration, and with two independent bilayers in the simulation box resulted in slower formation of a ripple structure.

2D angle-resolved WAXS spectra calculated for three different ripple structures are shown in Fig. 3. The first is a finished DPPC ripple structure, showing ordering in both *M* and *m* domains (Fig. 3*A*). The second is a DPPC ripple phase structure, showing an ordered *m* domain with interdigitated lipids, but with a partially melted *M* domain (Fig. 3*B*). This structure was formed after 0.5 ns of simulation at the elevated temperature of 313 K, starting from the completed ripple-phase structure. In the third structure, the *M* domain has formed, but the *m* domain is still liquid crystalline-like and only partly interdigitated (Fig. 3*C*). This structure is taken after 35 ns of a simulation run at 283 K, starting from the liquid crystalline state. It can be seen in Fig. 3 that the angle-resolved WAXS spectra exhibit clear peaks, consistent with the presence of material with short-range order. The pattern of the peaks is seen to depend on the nature and amount of ordered material. The completed ripple structure (Fig. 3*A*) shows the clearest peaks at $q_z \approx \pm 0.50$–0.40, $q_r \approx 1.45$–1.50 Å^{-1}. Strong, broad peaks in the region $q_z \approx \pm 0.35$–0.15, $q_r \approx 1.40$–1.55 Å^{-1}, are found for the structure with the partially melted *M* domain but with the *m* domain still fully interdigitated (Fig. 3*B*). The WAXS spectrum of the structure with the ordered *M* domain but the liquid-like *m* domain (Fig. 3*C*) shows considerably weaker peaks, which are furthermore strongest on the line $q_z \approx 0$ Å^{-1} around $q_r \approx 1.52$ Å^{-1}.

Discussion

The simulations give ripple characteristics for DPPC (Fig. 1) in the following range: λ_r, 12–16 nm; d, ≈6.5 nm; γ, 56–118°; x_0 (projection of *M* domain on ripple vector), 9–10 nm; and A (ripple amplitude), ≈2.4 nm. These dimensions of the ripple are consistent with the available experimental data. Ripple characteristics for DPPC are not known in such detail as given here. They depend on hydration level and temperature and are found in the range: λ_r, 13.4–20 nm; d, 6.2–7.2 nm; γ, 88–98°; d_l, 4.5–4.9 nm; d_w, 1.3–2.3 nm (5, 7), where d_l and d_w are the average thicknesses of the lipid and water layers, respectively. A detailed study of the thicknesses of the lipid and water layers in the different domains of the ripple was undertaken only for dimyristoylphosphatidylcholine (DMPC) (6). For DMPC, d_M was given as 3.8 nm, w_M was 2.1 nm, d_m was 3.1 nm, and w_m was 1.8 nm. For the simulation of DPPC shown in Fig. 2, we find d_M is 4.6 nm, w_M is 2.1 nm, d_m is 3.2 nm, and w_m is 4.8 nm. Given that the acyl chains of DPPC are two methylene units longer than those of DMPC, our DPPC results are consistent with those of

DMPC. Discrepancies with experimentally based descriptions of the ripple phase structure occur largely in the oblique angle γ and in the thickness of the water layer between the *m* domains (w_m). This finding may be explained by the fact that under experimental conditions excess water can sequester into a separate phase, whereas in the simulations the water is restricted to the simulation box and can sequester most effectively by changing the oblique angle γ. Furthermore, γ, w_M, and w_m are coupled (7). Simulations at lower hydration show that w_M remains the same, whereas w_m decreases. At very low hydration, a ripple structure does not form. Instead, a tilted gel phase ($L_{\beta'}$) is formed (Fig. 7, which is published as supporting information on the PNAS web site), in accordance with experiment. The simulation temperatures at which ripple structures were formed are below the experimental pretransition temperature of 308 K at full hydration (5), and it may be argued that the formation of a ripple structure should not have been observed. It should be noted, however, that the true temperature in a molecular simulation is not defined precisely because the states sampled during a simulation are determined by their relative Boltzmann weights. Temperature enters the Boltzmann equations as a scaling factor, and thus the absolute temperature of the system cannot be defined independently of the force field. Slight inadequacies in the force field will be manifest as slight shifts in the calculated phase diagram with respect to the experimentally determined phase diagram. It is only by modeling temperature-sensitive thermodynamic properties such as phase transitions that the absolute temperature of a simulation performed by using a specific force field can be determined. In addition, the time required for the process of phase transformation to take place strongly depends on how much below the phase transition temperature the simulation is performed. The investigations were performed at a temperature well below the expected transition temperature to keep the simulations tractable.

Perhaps the most salient feature of the ripple structure seen in the simulations is the complete interdigitation of the acyl chains in the *m* domain. Interdigitation of phosphatidylcholine lipids has been described extensively in the literature (27), but has only been speculated about in conjunction with the ripple phase of single-component phosphatidylcholines by Wack and Webb (5). Laggner *et al.* (28) proposed a ripple structure with an interdigitated domain formed by dihexadecylphosphatidylcholine (DHPC) lipids for mixed systems of DPPC and DHPC. In DHPC the tails of the lipids are linked to the glycerol backbone through ether links, rather than through ester links as in DPPC. Interdigitation of lipids provides an efficient mechanism for combining a high degree of tail ordering (a characteristic of gel states) with a high level of hydration of the head groups (a characteristic of the liquid crystalline state).

Interdigitation does not appear to arise as an artifact of the force field or the simulation conditions. An uninterdigitated gel phase is stable at temperatures below the pretransition temperature, and from this gel phase the ripple phase with an interdigitated domain is formed spontaneously upon raising the temperature. Raising the temperature starting from the ripple phase structures in turn leads to the L_α state. Also, interdigitation is not seen when simulating bilayers of phosphatidylethanolamine lipids at temperatures below their transition temperature (Fig. 7). The phosphatidylethanolamine head group is smaller than the PC head group and it is well known that dipalmitoylphosphatidylethanolamine (DPPE) and dilauroylphosphatidylethanolamine (DLPE) lipids do not form ripple phases. Instead, in simulations of DPPE and DLPE bilayers we find L_β structures for these lipids, in accordance with experimental data (29, 30).

The ripple structures found in the simulations contain a significant fraction ($\approx$10%) of lipids with disordered tails. Several techniques have suggested such a feature (11, 12, 14), and this finding has fueled speculation that the minor domain is L_α-like. All lipids with highly disordered tails in our simulation were found in the kink regions. Analysis of the mobility of the lipids showed that the lipids in the kink regions are much more mobile than the lipids in the ripple leg regions. They behave as if they are in a restricted fluid phase with clear long-range diffusion. This finding is consistent with results from fluorescence photobleaching recovery experiments (14).

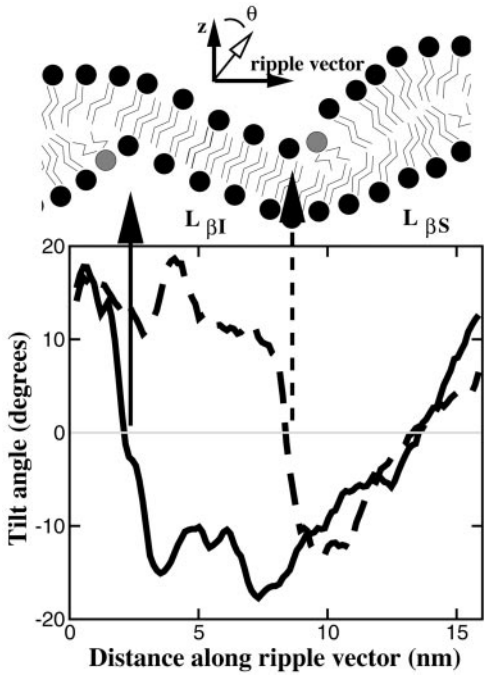

Fig. 4. Tilt of lipids in the ripple phase. (*Upper*) A schematic representation of the organization of the lipids in the ripple structure. (*Lower*) The tilt angle of the tails of the lipids with respect to the overall ripple normal (the *z* axis) is shown as a function of position along the ripple vector. The tilt angles of the chains in the two leaflets of the bilayer are shown separately. The dotted line corresponds to the upper leaflet; the drawn line corresponds to the lower leaflet. Clearly shown are the reversal of the tilt angle along the ripple vector in each monolayer at one end of the kink region (indicated by arrows) and the splay in the gel-like domain (gradual change in tilt angle between 10 and 16 nm). The parallel arrangement of the chains in the interdigitated region (between 3 and 8 nm) is also clearly visible. The tilt angle is defined as the angle between the vector connecting the fourth and 12th carbon atoms in each DPPC tail and the *z* axis. The data are calculated from a representative simulation of the DPPC ripple phase.

The organization of the lipids as seen in our simulations supports the theory (9) that packing competition between the head groups and tails in phosphatidylcholine lipids leads to the formation of a rippled phase. In particular, the occurrence of splay predicted by this theory is clearly visible in Fig. 2*C*. Splay leads to packing frustration between two neighboring splayed domains, visible in Fig. 2*B*. The packing frustration may be relieved by there being disordered material in between the ordered domains. Interdigitation has not been proposed in any theory of the ripple phase, but the introduction of a tilted, interdigitated domain between two splayed domains is an effective way to increase the amount of ordered material while minimizing the amount of disordered material required to enable the sudden change in the orientation of the chains required to start a new splayed domain. A cartoon of the organization of the lipids in the ripple phase as found in our simulations is shown in Fig. 4, together with the observed tilt angles of the lipids with respect to the stacking direction along the ripple vector. The interdigitated domain facilitates a con-

tinuous gel structure by transferring the splay from one monolayer to the other (Figs. 2*C* and 4). The organization of the lipids in this splayed gel structure with continuously changing tilt angle along the ripple vector is quite distinct from that in the L_{β}' phase in which the tilt angle of the lipids is uniform. We therefore suggest the notation $L_{\beta S}$ to characterize such a splayed gel phase. The ripple structure proposed here is similar to the structure proposed by Laggner *et al.* (28) for the mixed DPPC/dihexadecylphosphatidylcholine systems, but differs from it in two important aspects. First, there are a substantial number of disordered lipids. Second, the gel is splayed. Interaction between two neighboring bilayers also plays a role in the formation of the ripple phase because it is not formed at very low hydration (5, 9). Our simulations suggest that the formation of splayed gel domains is suppressed at very low hydration, presumably because of the repulsion between the bilayers. Instead, uniformly tilted gel domains are formed, resulting in an L_{β}' phase (Fig. 7).

The time scales involved in the formation of the ripple phase in the simulations are influenced by the temperature and the chain length. Higher temperatures and shorter chain lengths slow the formation of the ripple phase structure shown in Figs. 1 and 2. Lipid bilayers of dilauroylphosphatidylcholine were also seen to develop asymmetric ripple structures with interdigitated tails in the *m* domain when simulated at temperatures below that of the main phase transition temperature (Fig. 8, which is published as supporting information on the PNAS web site). The process of interdigitation of the lipid tails in the *m* domain appears to be slow compared to the formation of the *M* domain and the emergence of a ripple structure. This finding may explain some of the apparent variation in experimental data regarding the nature of the *m* domain.

Experimental verification of the proposed structure should be possible by measuring angle-resolved WAXS spectra of ordered stacks. Calculated WAXS spectra of ripple structures with and without an interdigitated, ordered *m* domain clearly show absorption at different positions in q_z-q_r space (Fig. 3). It is the interdigitated, ordered *m* domain that causes intense WAXS peaks. The fact that the WAXS peak in powder spectra of the ripple phase is even sharper than the WAXS peak of the gel phase, as reported by Cunningham *et al.* (13), may be interpreted as lending support to a ripple phase structure with a high degree of short-range order.

In summary, MD simulations of spontaneously formed rippled bilayer structures for phosphatidylcholine lipids showed that the organization of lipid molecules in the lecithin ripple phase (P_{β}') is gel-like and not interdigitated with a continuously changing lipid tilt angle along the ripple vector in the *M* domain ($L_{\beta S}$), whereas in the *m* domain the lipid tails are fully interdigitated, resembling the ($L_{\beta I}$) phase. Lipids in the kink regions between the domains are highly disordered and significantly more mobile than lipids in the ordered *M* and *m* domains. The proposed structure is consistent with all available data and can be verified by using WAXS on ordered stacks.

We thank John Nagle, Wilfred van Gunsteren, and Herman Berendsen for supportive and constructive discussions and careful reading of the manuscript. Financial support from MSC_{plus} is gratefully acknowledged.

1. Nagle, J. F. & Tristram-Nagle, S. (2000) *Biochim. Biophys. Acta* **1469,** 159–195.
2. Simons, K. & Ikonen, E. (1997) *Nature* **387,** 569–572.
3. Koynova, R. & Caffrey, M. (1998) *Biochim. Biophys. Acta* **1376,** 91–145.
4. Tardieu, A., Luzzati, V. & Reman, F. C. (1973) *J. Mol. Biol.* **75,** 711–733.
5. Wack, D.C. & Webb, W. W. (1989) *Phys. Rev. A* **40,** 2712–2730.
6. Sun, W.-J., Tristram-Nagle, S., Suter, R. M. & Nagle, J. F. (1996) *Proc. Natl. Acad. Sci. USA* **93,** 7008–7012.
7. Katsaras, J., Tristram-Nagle, S., Liu, Y., Headrick, R. L., Fontes, E., Mason, P. C. & Nagle, J. F. (2000) *Phys. Rev. E* **61,** 5668–5677.
8. Sengupta, K., Raghunathan, V. A. & Katsaras, J. (2003) *Phys. Rev. E* **68,** 031710.
9. Carlson, J. M. & Sethna, J. P. (1987) *Phys. Rev. A* **36,** 3359–3374.
10. Tristram-Nagle, S. & Nagle, J. F. (2004) *Chem. Phys. Lipids* **127,** 3–14.
11. Cameron, D. G., Casal, H. L. & Mantsch, H. H. (1980) *Biochemistry* **19,** 3665–3672.
12. Wittebort, R. J., Schmidt, C. F. & Griffin, R. G. (1981) *Biochemistry* **20,** 4223–4228.
13. Cunningham, B. A., Brown, A.-D., Wolfe, D. H., Williams, W. P. & Brain, A. (1998) *Phys. Rev. E* **58,** 3662–3672.
14. Schneider, M. B., Chan, W. K. & Webb, W. W. (1983) *Biophys. J.* **43,** 157–165.
15. Scott, H. L. (2002) *Curr. Opin. Struct. Biol.* **12,** 495–502.
16. Tu, K., Tobias, D. J., Blasie, J. K. & Klein, M. L. (1996) *Biophys. J.* **70,** 595–608.
17. Venable, R. M., Brooks, B. R. & Pastor, R. W. (2000) *J. Chem. Phys.* **112,** 4822–4832.
18. Kranenburg, M., Laforge, C. & Smit, B. (2004) *Phys. Chem. Chem. Phys.* **6,** 4531–4534.
19. Anézo, C., de Vries, A. H., Höltje, H.-D., Tieleman, D. P. & Marrink, S. J. (2003) *J. Phys. Chem. B* **107,** 9424–9433.
20. Tironi, I. G., Sperb, R., Smith, P. E. & van Gunsteren, W. F. (1995) *J. Chem. Phys.* **102,** 5451–5459.
21. Lindahl, E., Hess, B. & van der Spoel, D. (2001) *J. Mol. Mod.* **7,** 306–317.
22. Berendsen, H. J. C., Postma, J. P. M., van Gunsteren, W. F., DiNola, A. & Haak, J. R. (1984) *J. Chem. Phys.* **81,** 3684–3690.
23. Parrinello, M. & Rahman, A. (1981) *J. Appl. Phys.* **52,** 7182–7190.
24. Hoover, W. G. (1985) *Phys. Rev. A* **31,** 1695–1697.
25. Marrink, S. J., Lindahl, E., Edholm, O. & Mark, A. E. (2001) *J. Am. Chem. Soc.* **123,** 8638–8639.
26. de Vries, A. H., Mark, A. E. & Marrink, S. J. (2004) *J. Am. Chem. Soc.* **126,** 4488–4489.
27. Slater, J. L. & Huang, C.-H. (1988) *Prog. Lipid Res.* **27,** 325–359.
28. Laggner, P., Lohner, K., Degovics, G., Müller, K. & Schuster, A. (1987) *Chem. Phys. Lipids* **44,** 31–60.
29. McIntosh, T. J. & Simon, S. A. (1986) *Biochemistry* **25,** 4948–4952.
30. Tenchov, B., Koynova, R. & Rapp, G. (2001) *Biophys. J.* **80,** 1873–1890.

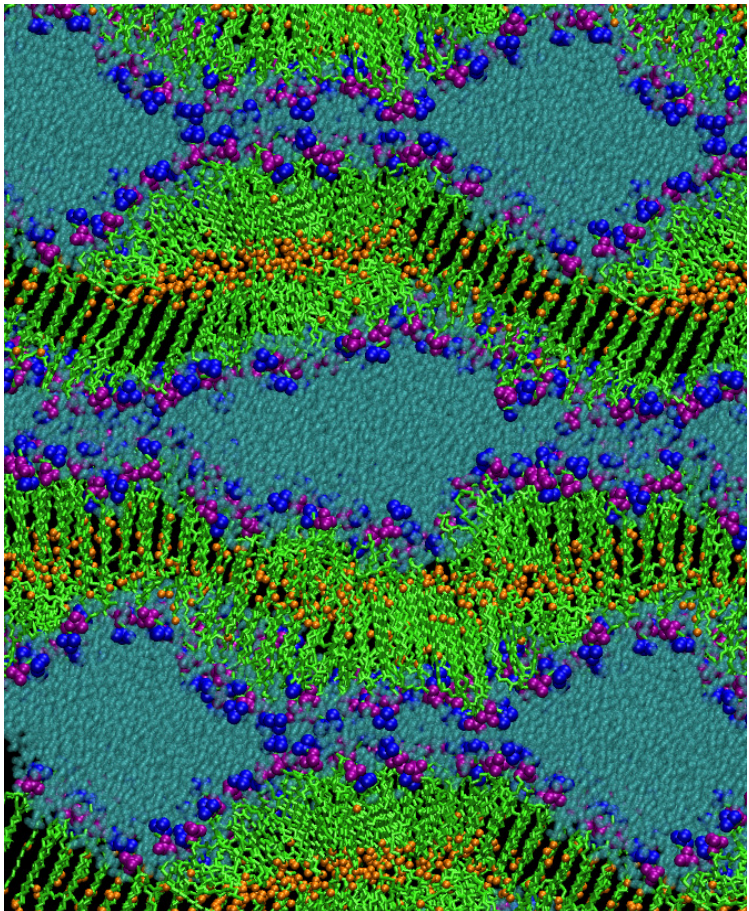

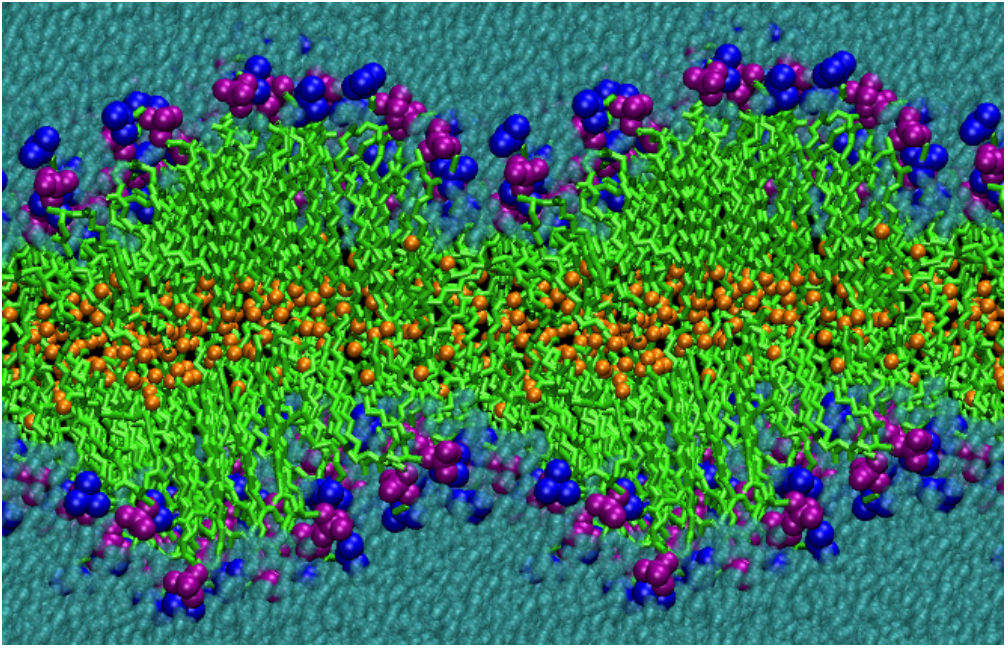

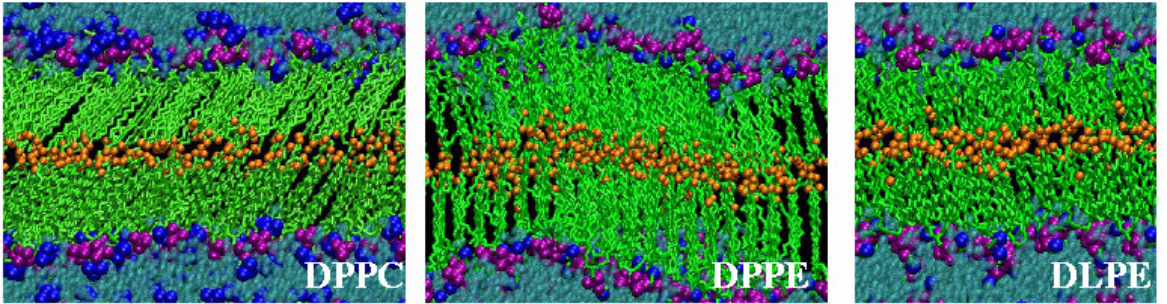
DPPC
DPPE
DLPE